

Note

Corrosion failure analysis of duplex stainless steel in marine environment

Haipeng Wang¹, Yang Yang¹, Zhongna Yang¹, Zhigang Xu¹, Yuanyuan Chai², Zhuwu Zhang^{3,*}

¹ CNOOC (Tianjin) Pipeline Engineering Technology Co., Ltd., Tianjin, 300452, China

² Tianjin Jiu Environment Testing Co., Ltd., Tianjin, 300452, China

³ College of Chemical Engineering, Fuzhou University, Fuzhou, 350116, China

*E-mail: zwzhang@fzu.edu.cn

Received: 7 December 2021 / Accepted: 31 December 2021 / Published: 5 April 2022

Serious crevice corrosion was detected at wear ring and pump casing of an S32760 duplex stainless steel fire pump assembled on an offshore platform, which resulted in broken of the wear ring. The failure mechanism of the cracked wear ring was analyzed, and results showed that the chemical composition of the wear ring corresponds to the standard S32760. However, metallographic test results showed that the wear ring has many harmful σ -phases and inclusions in the matrix, which led to the decrease of corrosion resistance of the material and induced crevice corrosion at the bolt joint and the wear ring. Besides, Chloride, sulfide, sodium and potassium have been found at corrosion products and pump casing fragments through energy dispersive X-ray spectrometry. Thus, to extend the service life of the fire pump, better sealing measures are needed to prevent crevice corrosion.

Keywords: S32760; stainless steel; crevice corrosion; fire pump; X-ray spectrometry

1. INTRODUCTION

The austenite-ferrite duplex stainless steel is widely used on marine equipment due to its excellent mechanical property and corrosion resistance. The duplex stainless steel has higher chloride stress corrosion resistance than other steels, which is beneficial to prevent intergranular corrosion and pitting corrosion caused by seawater corrosion [1-6]. Complex corrosive factors in a marine environment, such as bacterial corrosion and chlorine element, become the focus of present research on duplex stainless steel. It has been confirmed that iron-oxidizing bacteria can lead to crevice corrosion of stainless steel. For duplex stainless steel, it is found that the duplex stainless steel would occur localized corrosion caused by a high concentration of Cl, K and Na in the biofilm structures from the enzymatic activities of halophilic bacterium [7]. The localized corrosion also would occur due to

the passive film on the surface of stainless steel destroyed by the chlorine in seawater. Besides, the dissolution rate of metal in local corrosion areas is significantly higher than that in other areas [8-10].

In this study, the crevice corrosion mechanism of an S32760 duplex steel fire pump in a marine environment was researched. Pump casing and wear ring, and cracked wear ring of the fire pump has been severely corroded. The corroded fire pump was placed on the offshore platform, and the corroded part was immersed in seawater. Macroscopic examination, detailed metallurgical investigation, chemical elements test, hardness test, and corrosion product test of the corroded wear ring were conducted [11-22]. The failure reasons have been revealed and better protective measures have been suggested.

2. EXPERIMENTAL METHODS

The samples in this work were cut from two parts (i.e. the most severely corroded parts) of the failed fire pump: wear ring and pump casing, respectively. Macroscopic visual inspection was taken by Canon EOS 7D camera. The dimension data of failed parts were measured with a Vernier caliper and ruler.

The chemical composition of the failed wear ring was measured by SPECTRO LAB M11 spectrometer with a detection limit from 0.0002% to 0.003%. The minimum detectable limit of molybdenum was 0.0002%. And the minimum detectable limit of carbon, manganese, sulfur, chromium is 0.003%.

Microstructure and inclusion of the failed wear ring were detected using ZEISS observer A1m metallurgical microscope. The metallographic specimen cut from the intact part of the failed wear ring was used to examine the microstructure and inclusion. Aqua regia was chosen as a metallographic etchant to measure the microstructure. Inclusions were observed in the polished state.

Energy dispersive X-ray spectrometry (EDS) of ZEISS EVO 18 scanning electron microscope (SEM) was used to determine the composition of the corrosion product through point scanning mode.

3. RESULTS AND DISCUSSION

3.1. Macroscopic inspection

Fig. 1 shows the corrosion condition of the pump casing and the wear ring, and no obvious plastic deformation can be observed on them. As shown in Fig. 1 (a), the wear ring is assembled with the pump body by clearance fit, and the function of bolts is to prevent relatively sliding. A deep etch groove with a length of 100 mm is found at the flange (Fig. 1 (b)). More than half of the circumference of the wear ring has been corroded with varying degrees, and the largest corrosion depth reaches to 5 mm. The corroded wear ring cracks at the position of the corroded bolt hole as shown in Fig. 1 (c). An initial corrosion morphology of another bolt hole also can be found in Fig. 1 (d).

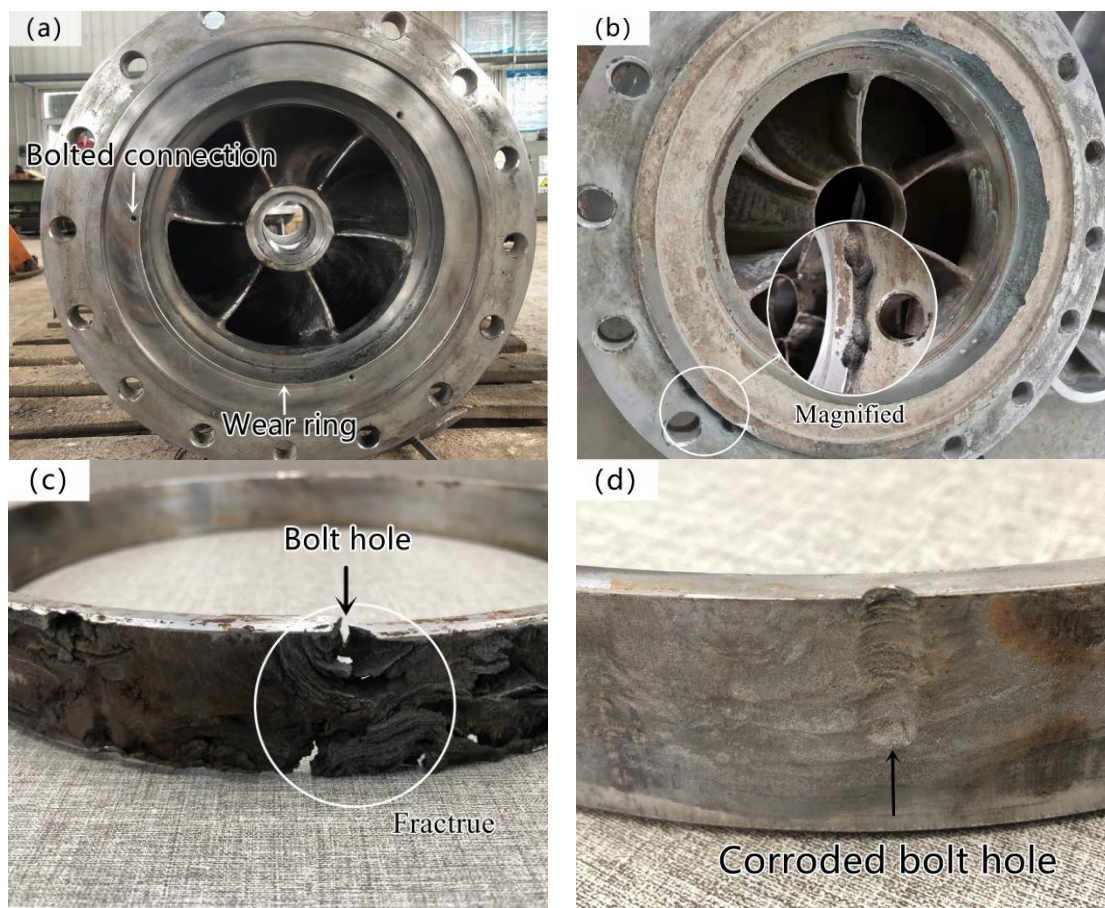


Figure 1. Pictures of the failed parts: (a) Intact pump casing with wear ring; (b) Corroded pump casing; (c) Corroded and cracked wear ring; (d) Corroded bolt hole on the ring.

3.2 Chemical composition

The chemical composition of the failed wear ring measured by SPECTRO LAB M11 spectrometer is listed in **Table 1**. It is found that the chemical composition of the wear ring corresponds to the requirement of standard S32760. However, pitting resistance equivalent (PRE = wt.% Cr + (3.3 * wt.% Mo) + (16 * wt.% N) of the wear ring is about 39.97% and lower than the requirement of standard S32760, i.e. 40.6%, which is easy to cause pitting corrosion of the wear ring [23].

Table 1. Chemical composition of failed wear ring (wt.%).

Sample	C	Si	Mn	N	P	S	Cr	Ni	Mo	Cu
Wear ring	0.0209	0.201	0.736	0.209	0.0243	0.0021	25.01	7.66	3.52	0.557
Standard S32760	0.03	1.00	1.00	0.2-0.3	0.03	0.01	24.00-26.00	6.0-8.0	3.0-4.0	0.5-1.0

3.3. Microstructure and inclusion

Fig. 2 shows the microstructure of the failed wear ring. It is found that the austenite phase presents two forms: the “island” austenite stretched along the rolling direction and thin strip austenite. And ferrite is located in the matrix around austenite. The proportion of austenite and ferrite is close to 1:1. Some sigma phase is found at the grain boundary of austenite and ferrite. As shown in **Fig. 3**, some inclusions of Al_2O_3 and $m\text{CaO}\cdot n\text{Al}_2\text{O}_3$ can be found in the polished metallographic specimen.

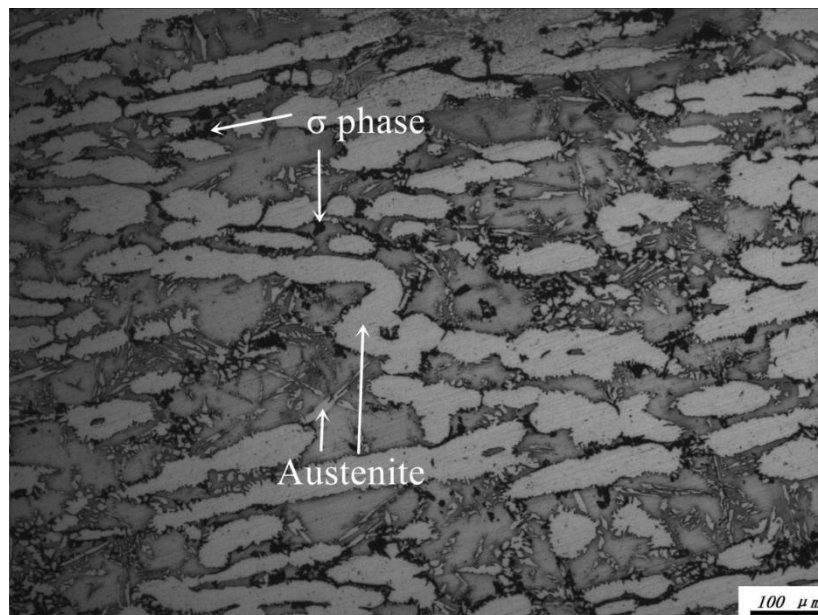


Figure 2. Microstructure of the failed wear ring.

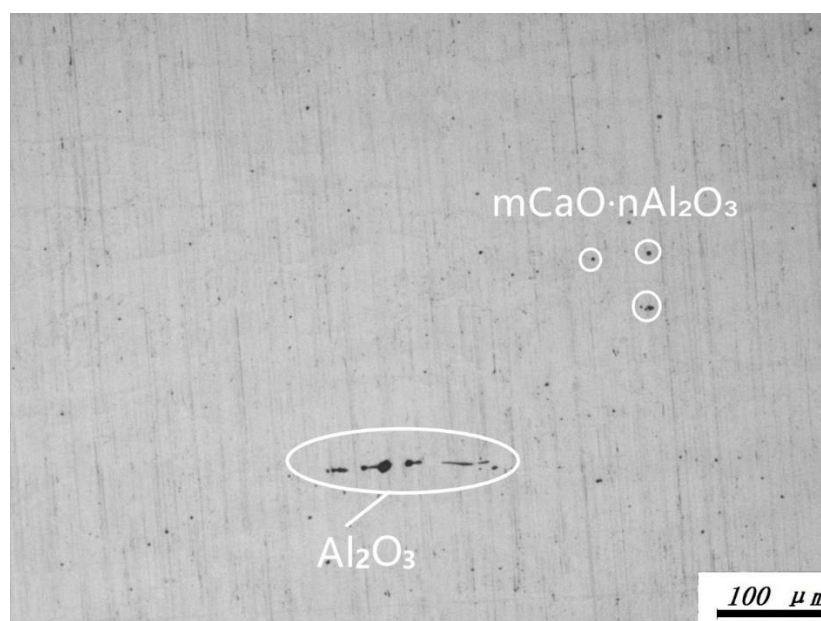


Figure 3. Inclusions of the failed wear ring.

3.4. SEM and EDS testing results

The chemical compositions of corrosion products and pump casing fragments near the crevice side were tested by EDS (**Figs. 4 and 5**). As listed in **Tables 2 and 3**, the results show that all the corrosion products obtained from both the failed wear ring and pump casing contain chloride, which increases the possibilities of pitting corrosion and crevice corrosion of stainless steel. And the chlorine reaggregated in the crevice is a typical feature of crevice corrosion [24].

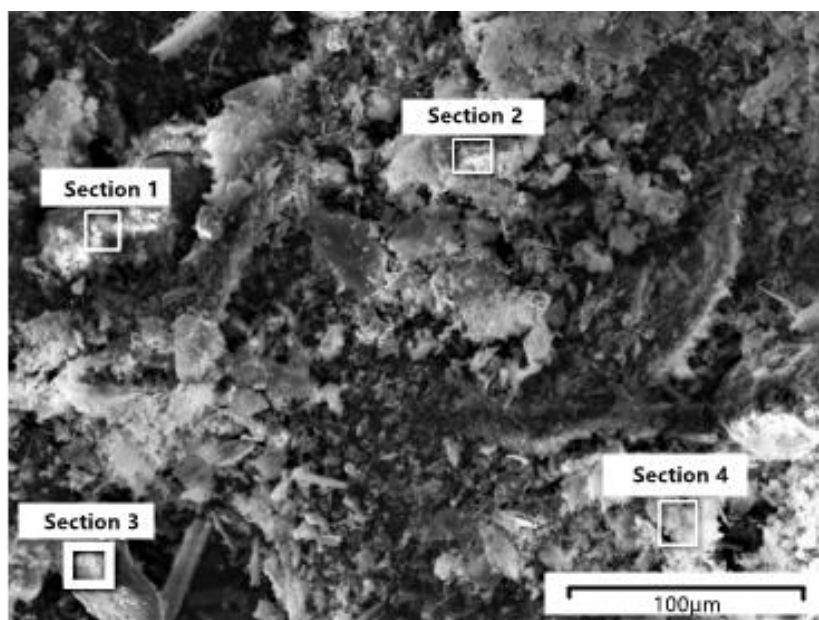


Figure 4. EDS testing sections of corrosion products.

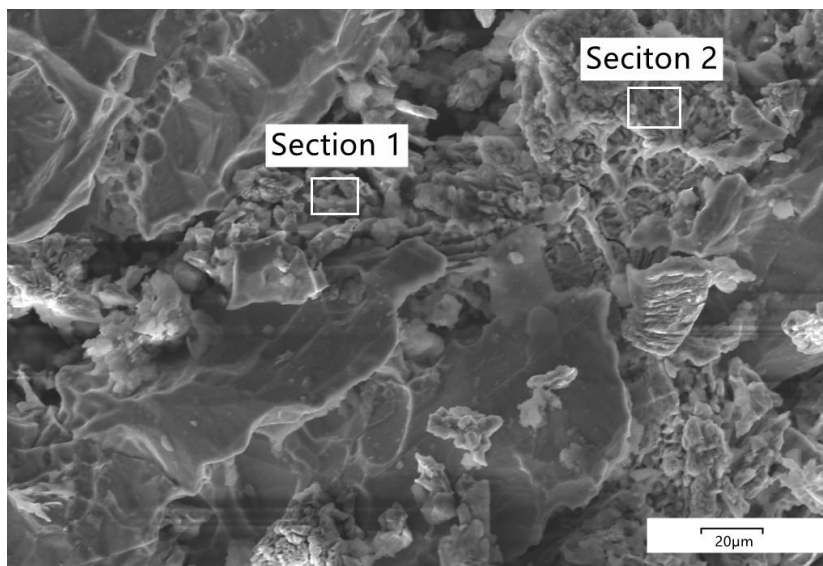


Figure 5. EDS testing sections of pump casing fragments.**Table 2.** Chemical compositions of corrosion products by EDS (wt.%).

Section	C	Fe	Na	Mg	Si	Al	Cl	S	O	Cr	Mn	Cu	Ca	K
1	/	0.99	7.52	0.60	31.73	2.76	12.44	0.46	40.13	0.95	/	1.44	/	0.97
2	6.16	18.08	8.35	0.34	16.74	/	8.72	0.61	23.66	13.81	0.32	0.86	0.11	0.14
3	9.48	44.49	1.22	0.27	6.18	0.27	0.83	0.57	10.88	18.54	0.90	0.94	0.14	/
4	10.31	3.92	4.61	0.35	27.20	0.41	5.66	0.65	40.60	4.37	/	0.75	0.28	0.28

Table 3. Chemical compositions of pump casing fragments by EDS (wt.%).

Section	C	Fe	Na	Si	K	Al	Cl	O	Cr	Mn	Ni	Mo
1	5.14	49.22	0.26	0.81	0.31	0.26	0.30	1.28	32.30	1.06	1.44	4.59
2	32.76	29.72	0.94	0.13	/	0.15	0.18	8.31	18.61	0.51	2.29	/

3.4. Discussion

According to the macroscopic inspection, all the corrosion positions of this fire pump occur in crevices, such as the crevice caused by clearance fit of wear ring and pump casing or the bolt crevice. Based on the EDS results, corrosion products contain a large amount of chloride indicating that the failure mechanism of the fire pump is crevice corrosion in the marine environment [25-27].

Although the chemical compositions of the failed wear ring correspond to the standard S32760 (Table 1), the matrix of the wear ring contains many harmful σ -phases according to the metallographic testing results. The stainless steel would occur compositional segregation caused by the σ -phases inducing that chromium and molybdenum at grain boundary are depleted, which is easy to cause intergranular corrosion resistance and pitting corrosion [28, 29]. The existence of inclusions destroys the continuity of matrix structure and causes uneven chemical composition, which leads to selective corrosion [30]. Inclusions and σ -phase precipitates are potential sensitive corrosion areas.

The condition for crevice corrosion is that corrosive medium enters and stays in the crevice, thus the crevice width is usually between 0.025-0.1 mm. Besides, it is proved that when the crevice width is 0.1-0.15 mm, crevice corrosion sensitivity is the highest and the corrosion rate is the most serious [31]. It is easy to form crevices with different widths at the flange, wear ring and bolt attributing to non-uniform stress and the difference of surface conditions in the assembling process.

Fig. 6 shows procedures of crevice corrosion of the fire pump. At first, the reaction rate of the cathode in the crevice is the same as that of the anode. However, with the development of corrosion, the corrosion current density of the anode is greater than that of the cathode due to oxygen consumption in the crevice. Then, because of the increase of ferric ion (Fe^{2+}) in the crevice, chloride ion (Cl^-) is transferred to the inside crevice for maintaining charge balance. Thus, the hydrolysis

tendency of Fe^{2+} will be enhanced due to the increase of Cl^- in the crevice, which leads to the decrease of pH value in the crevice increasing corrosion rate and resulting in the wear ring crack.

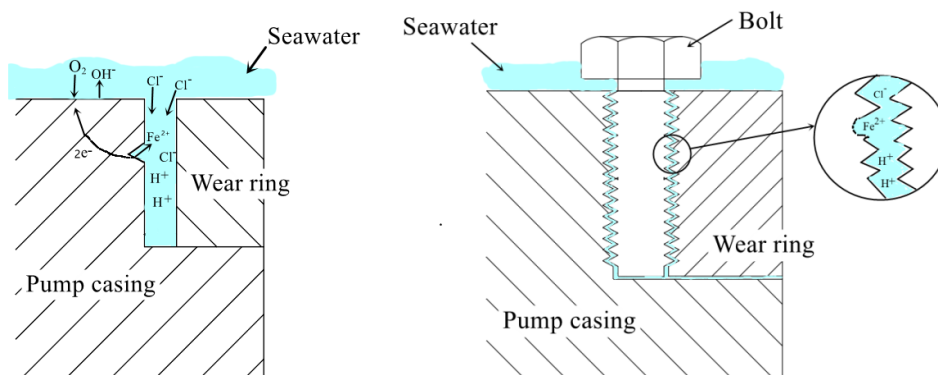
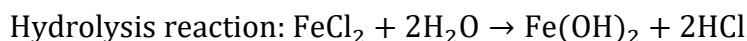
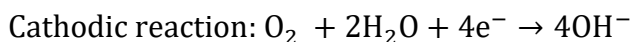


Figure 6. Schematic diagram of crevice corrosion.

4. CONCLUSIONS

It is easy for seawater to penetrate the existence of crevices at the bolt joint and the wear ring, inducing the crevice corrosion that results in corrosion fracture of the fire pump. Although the chemical compositions of the failed wear ring correspond to the standard S32760, σ -phase is found at the grain boundary between austenite and ferrite resulting in the compositional segregation. Besides, the depletion of chromium and molybdenum at the grain boundary caused by the σ -phase easily leads to intergranular corrosion and pitting corrosion.

Thus, to extend the service life of the fire pump, better sealing measures are needed to prevent crevice corrosion.

References

1. K. M. Adhe, V. Kain, K. Madangopal, H. S. Gadiyar, *J. Mater. Eng. Perform.*, 5 (1996) 500.
2. G. Kear, B. D. Barker, F. C. Walsh, *Corrosion*, 60 (2012) 561.
3. M. Baxmann, S. Y. Jauch, C. Schilling, W. Blmer, *Met. Eng. Phys.*, 35 (2013) 676.
4. A. I. Muñoz, J. G. Antón, S. L. Nuévalos, J. L. Guiñón, V. P. Herranz, *Corros. Sci.*, 46 (2004) 2955.
5. El-Sayed M. Sherif, J. H. Potgieter, J. D. Comins, L. Cornish, P. A. Olubambi, C. N. Machio, *Corros. Sci.*, 51 (2009) 1364.
6. Z. W. Yu, X. L. Xu, *Mater. Charact.*, 59 (2008) 192.
7. Z. H. Sun, M. Moradi, Y. X. Chen, R. Bagheri, P. S. Guo, L. J. Yang, Z. L. Song, C. Xu, *Mater. Chem. Phys.*, 208 (2018) 149.

8. N. Larché, D. Thierry, V. Debout, J. Blanc, T. Cassagne, J. Peultier, E. Johansson, C. Taravel-Condât, *Rev. Metall.*, 108 (2012) 451.
9. R. A. Perren, T. A. Suter, P. J. Uggowitz, L. Weber, R. Magdowski, H. BöHni, M. O. Speidel, *Corros. Sci.*, 43 (2001) 707.
10. Y. Z. Yang, Y. M. Jiang, J. Li, *Corros. Sci.*, 76 (2013) 163.
11. H. Baba, T. Kodama, Y. Katada, *Corros. Sci.*, 44 (2002) 2393.
12. B. Ananya, M. Singh Preet, *J. Fail. Anal. Prev.*, 7 (2007) 371.
13. L. F. Garfias-Mesias, J. M. Sykes, C. D. S. Tuck, *Corros. Sci.*, 38 (1996) 1319.
14. S. H. Jeon, S. T. Kim, L. S. Lee, Y. S. Park, *Corros. Sci.*, 52 (2010) 3537.
15. F. J. Martin, K. E. Lucas, E. A. Hogan, *Rev. Sci. Instrum.*, 73 (2002) 1273.
16. M. Edward. *Mechanically Assisted Corrosion*, Springer New York, (2010) New York.
17. H. W. Pickering, *Corrosion*, 42 (1986) 125.
18. H. W. Pickering, *Corros. Sci.*, 29 (1988) 325.
19. H. W. Pickering, K. Cho, E. Nystrom, *Corros. Sci.*, 35 (1993) 775.
20. B. Popov. *Corrosion Engineering*, (1986) New York.
21. P. A. Thornton, *J. Mater. Sci.*, 6 (1971) 347.
22. S. Azuma, H. Tsuge, T. Kudo, T. Moroishi, *Corros. Sci.*, 45 (1989) 235.
23. G. Baylac, J. M. Grandemange, *Nucl. Eng. Des.*, 129 (1991) 239.
24. J. Riskin, A. Khentov. *Electrocorrosion and Protection of Metals*, (2019) Amsterdam.
25. H. Cheshideh, F. Nasirpouri, B. Mardangahi, A. Jabbarpour, *Eng. Fail. Anal.*, 122 (2021) 105240.
26. L. B. Niu, K. Okano, S. Izumi, K. Shiokawa, M. Yamashita, Y. Sakai, *Corros. Sci.*, 132 (2018) 284.
27. O. P. Calabokis, Y. N. Rosa, C. M. Lepienski, R. P. Cardoso, P. C. Borges, *Surf. Coat. Tech.*, 413 (2021) 127095.
28. J. Li, X. Ren, Y. Zhang, H. Hou, X. Gao, *Prog. Nat. Sci.: Mater. Int.*, 31 (2021) 334.
29. D. D. S. Silva, T. A. Simões, D. A. Macedo, A. H. S. Bueno, S. M. Torres, R. M. Gomes, *Mater. Chem. Phys.*, 259 (2021) 124056.
30. F. Ning, J. Tan, Z. Zhang, X. Wu, X. Wang, E. H. Han, W. Ke, *J. Mater. Sci. Technol.*, 66 (2021) 163.
31. I. L. Rosenfeld, K. W. Staehle, *Corros. Eng., Sci. Technol.*, 1 (1974) 325.